Fish and Shellfish Immunology 93 (2019) 484–491

Contents lists available at ScienceDirect

Fish and Shellfish Immunology

journal homepage: www.elsevier.com/locate/fsi

Short communication

Molecular cloning and modeling of the Tp53-induced glycolysis and apoptotic regulator (TIGAR) from the Pacific white shrimp *Litopenaeus vannamei* and its expression in response to hypoxia

Laura Camacho-Jiménez[a], Monserrath Felix-Portillo[b], Dahlia M. Nuñez-Hernandez[a], Gloria Yepiz-Plascencia[a,*]

[a] Centro de Investigación en Alimentación y Desarrollo (CIAD), A.C, Carretera Gustavo Enrique Astiazarán Rosas, no. 46, col La Victoria, Hermosillo, Sonora, C.P. 83304, Mexico

[b] Facultad de Zootecnia y Ecología, Universidad Autónoma de Chihuahua, Periférico Francisco R. Almada, Km 1, Chihuahua, Chihuahua, 33820, Mexico

ARTICLE INFO

Keywords:
Gene expression
Hypoxia
p53
Shrimp
TIGAR

ABSTRACT

Hypoxia is a common stressor for aquaculture species. The Pacific white shrimp *Litopenaeus vannamei* survives low dissolved oxygen (DO) conditions by adjusting its energy metabolism. In vertebrates, the transcription factor p53 regulates glucose metabolism under stress through diverse target genes like the Tp53-induced glycolysis and apoptotic regulator (TIGAR), a protein similar to fructose-2,6-bisphosphatase that has a pro-survival role in cells participating in the defense against oxidative damage. Until now, TIGAR has been not reported in any invertebrate species, including crustaceans. In this work, we report the molecular cloning of the white shrimp TIGAR. The cDNA sequence is 765 bp encoding a 254 amino acid protein. Bioinformatics analyses predicted that although the overall sequence identities of *L. vannamei* TIGAR and vertebrate proteins are not very high (33.61%–35.34%), they have a remarkable predicted structural similarity with full conservation of catalytic residues, secondary and three-dimensional structures. Gene expression analysis by RT-qPCR revealed that the mRNA abundance of TIGAR in white shrimp is tissue-specific under normal oxygen conditions, with higher expression in gills than hepatopancreas and muscle. Also, gene expression in gills and hepatopancreas is modified by environmental hypoxia, suggesting that TIGAR participates in the cellular tolerance of *L. vannamei* to this stressor.

1. Introduction

In aquatic ecosystems, dissolved oxygen (DO) concentrations less than 2 mg L^{-1} are considered as environmental hypoxia [1], a common situation that also occurs in aquaculture. Hypoxia in culture ponds is prompted by high stocking densities, poor aeration, increased respiration of photosynthesizers during hours of darkness, microbial decomposition of organic matter, among others [2]. Severe or persistent drops in dissolved oxygen can lead to massive mortalities of farmed organisms, but some commercially-important invertebrates like the Pacific white shrimp *Litopenaeus vannamei* are able to tolerate episodic DO concentrations lower than 1 mg L^{-1} [3]. Nonetheless, like any stressor, environmental hypoxia has negative effects on shrimp production including lower growth, reduced resistance to diseases, and higher mortality rates [4].

Hypoxia-tolerant animals have developed biochemical and molecular strategies to survive sub-optimal oxygen concentrations. When intracellular oxygen becomes limiting, energy production by oxidative phosphorylation is reduced, and anaerobic glycolysis is preferentially used for energy production [5]. In *L. vannamei*, as in most of tolerant species, acceleration of anaerobic glycolysis occurs through the tissue-specific induction of some enzymes that are transcriptionally regulated by the hypoxia inducible factor (HIF-1), an oxygen-sensitive transcription factor [6–11]. This response contributes to the establishment of a hypo-metabolic state, in which the limited ATP production by anaerobic metabolism is equilibrated with the reduction of ATP-demanding processes in cells to prevent lethal energy declines [12].

In addition to HIF-1, the tumor suppressor protein p53 (Tp53) is gaining attention as a mediator of the cellular response to hypoxia [13]. p53 is a stress-sensitive transcription factor with better-known roles in DNA repair, cell-cycle arrest, senescence and apoptosis [14]. The p53 expression is responsive to hypoxia in crustaceans like the prawn

* Corresponding author.
E-mail address: gyepiz@ciad.mx (G. Yepiz-Plascencia).

https://doi.org/10.1016/j.fsi.2019.08.003
Received 17 May 2019; Received in revised form 31 July 2019; Accepted 1 August 2019
Available online 01 August 2019

Macrobrachium nipponense [15] and *L. vannamei* [16,17], participating in apoptosis and/or cell-cycle control. In vertebrates, p53 also regulates glucose metabolism through diverse target genes [18]. One of these genes encodes the Tp53-induced glycolysis and apoptotic regulator (TIGAR), a protein with structural similarity to the bisphosphatase domain of the regulatory enzyme 6-phosphofructo-2-kinase/fructose-2,6-bisphosphatase (PFK-2/FBPase-2) [19]. Like FBPase-2, TIGAR hydrolyzes fructose-2,6-bisphosphate (Fru-2,6-P_2), an allosteric activator of the glycolytic enzyme phosphofructokinase 1 (PFK-1) [20]. Breakdown of Fru-2,6-P_2 results, in general, in suppression of glycolysis with consequences in survival relying on the cell-type, source of stress, and energy status of the cells [21]. Depending on the situation, the TIGAR-mediated reduction in glycolytic rate promotes apoptosis, but also can act as pro-survival response by redirecting carbohydrate flux to the pentose phosphate pathway (PPP) [19]. Increased PPP activity rises cellular pools of NADPH and reduced glutathione (GSH) used by antioxidant systems to neutralize reactive oxygen species (ROS) that are noxious for cells [22]. Nonetheless, in mammalian cells under hypoxia, for which the maintenance of a high glycolytic flux is prime for survival, TIGAR also promotes glycolysis by enhancing the activity of hexokinase (HK) in mitochondria [23].

The interest on TIGAR functions in vertebrates has been increasing since the first report by Bensaad et al. (2006). However, in "classic" invertebrate animal models like the fruit fly *Drosophila melanogaster* and the nematode worm *Caenorhabditis elegans* there is no conclusive evidence of a TIGAR homolog at gene or protein level [19]. Moreover, as far as we know, there are no studies reported about TIGAR in crustaceans or other aquatic invertebrates. In the present work, we report a complementary DNA (cDNA) sequence of *L. vannamei* TIGAR, the *in silico* characterization of the deduced protein, and the tissue-specific effect of hypoxia in mRNA expression.

2. Material and methods

2.1. Animals and hypoxia challenge

Juvenile shrimp *L. vannamei* were obtained from a local farm in Sonora, Mexico, transported to the Laboratory of Marine Invertebrates Physiology of CIAD and maintained in 100 L fiberglass tanks filled with aerated seawater (28 °C, 35‰, 5 ± 0.5 mg L^{-1} of DO). The tanks were connected to a recirculation system in which seawater was purified through sand-filters, 5 mM and 10 mM bag filters, ozone treatment, and bag filters once again. Shrimp were daily fed with commercial diet (35% protein) corresponding to 3% of their wet weight. Feces and residual food were removed from the tanks, and water quality was monitored. The seawater of the recirculation system was fully exchanged each time that ammonia reached levels > 3.0 mg L^{-1}. The animals were maintained under these conditions before experiments.

For the hypoxia assay, two groups of 12 shrimp (12.5 ± 0.59 g) in intermolt stage were distributed in separated tanks (100 L). Three days later, the hypoxic treatment was initiated in one of the two tanks by bubbling nitrogen gas into seawater to reach a final DO concentration of 1.54 ± 0.28 mg L^{-1}. As control, the seawater in the other tank was kept in normal DO conditions (5.13 ± 0.11 mg L^{-1}). The DO was monitored each hour with a portable oximeter (YSI model 55, Yellow Spring, OH, USA) and adjusted by regulating the air or nitrogen supply when necessary. Four shrimp either in normoxia or hypoxia were sampled after 24 and 48 h of stress exposure. In each sampling procedure, ~100 mg of muscle, hepatopancreas and gills were dissected from each shrimp, individually placed in microcentrifuge tubes with 10 volumes of TRI reagent, and immediately frozen by tube-submersion in liquid nitrogen. Samples were stored at −80 °C before RNA isolation.

2.2. Cloning and sequencing of TIGAR cDNA

Using the BLAST tool (https://blast.ncbi.nlm.nih.gov/Blast.cgi), a putative TIGAR mRNA sequence was identified from a transcriptome shotgun assembly (TSA) from *L. vannamei* hepatopancreas annotated in the GenBank database (https://www.ncbi.nlm.nih.gov/genbank/) (GenBank accession no. GETD01036061) by aligning with the amino acid sequence of *Daphnia magna* TIGAR (GenBank accession no. KZS04264). The coding sequence (CDS) in the TSA was predicted using ORFfinder (https://www.ncbi.nlm.nih.gov/orffinder/) and was amplified from hepatopancreas cDNA by polymerase chain reaction (PCR) using the specific primers TIGARFw1 (5′-ATGAGACGTTCGCTTCCT GTA-3′) and TIGARRv1 (5′-TTAGAGATCCTTCAGGTGTTC-3′). The PCR mixture (25 μL) contained 12.5 μL of Hot Start Taq 2X Master Mix (New England BioLabs, Ipswich, MA, USA), 0.6 μM of each primer, and 1 μL of cDNA (corresponding to 25 ng of total RNA) as template. The cycling conditions were: 95 °C, 3 min (1 cycle); 95 °C, 30 s, 57.5 °C, 30 s, 72 °C 1 min (40 cycles); 72 °C, 10 min (1 cycle). The PCR product was cloned using the pGEM®-T Easy Vector System (Promega, Madison, WI, USA) and the TOP10 strain of *Escherichia coli*. Two clones were sequenced in both strands at the University of Arizona Genetics Core (UAGC).

2.3. Sequence and phylogenetic analyses of TIGAR protein

The amino acid sequence of *L. vannamei* TIGAR was deduced from the cDNA sequence with the Translate tool available in the Sequence Manipulation Suite (http://www.bioinformatics.org/sms2/translate.html). The molecular weight (MW) and isoelectric point (pI) of the protein were predicted using ProtParam (https://web.expasy.org/cgi-bin/protparam/protparam).

The predicted white shrimp TIGAR amino acid sequence was compared with proteins from other species by a multiple sequence alignment with Clustal Omega (https://www.ebi.ac.uk/Tools/msa/clustalo/) and graphically edited with BioEdit (v. 7.2.6.1). The sequences included in the analysis were those from the water flea *D. magna*, the isopod *Armadillidium vulgare* (GenBank accession no. RXG68141.1), the amphipod *Hirondellea gigas* (GenBank accession no. LAB70507.1), the zebra fish *Danio rerio* (GenBank accession no. NP_956485.1), the frog *Xenopus laevis* (GenBank accession no. NP_001089513.1), the mouse *Mus musculus* (GenBank accession no. NP_795977.1) and the human *Homo sapiens* (GenBank accession no. NP_065108.1). Conserved domains in aligned proteins were identified using HMMER web server (https://www.ebi.ac.uk/Tools/hmmer/) with the Pfam database (http://pfam.xfam.org/).

A phylogenetic analysis including diverse species was done using MEGA (7.0.26). Protein sequences were aligned using the Clustal method with complete deletion of gaps and missing data. A phylogenetic tree was then built by the Maximum likelihood (ML) method and the Jones-Taylor-Thornton (JTT) amino acid substitution model. Each tree node was constructed from 1000 bootstrap replicates and the tree was rooted to the TIGAR protein from the fungus *Aspergillus lentulus*.

2.4. Homology modeling of L. vannamei TIGAR

The three-dimensional (3D) structure of *L. vannamei* TIGAR was predicted by homology modeling with MODELLER (v.16) (https://salilab.org/modeller/). The template structure was selected by a BLAST alignment between the deduced white shrimp protein and the structures deposited in the Protein Data Bank (https://www.rcsb.org/). Taking into account the highest sequence identity, the human TIGAR structure (PDB: 3DCY, chain A) determined by X-ray diffraction (1.748 Å) was selected as template. The model was refined by optimizing hydrogen bonding network and energy minimization in the 3DRefine server (http://sysbio.rnet.missouri.edu/3Drefine/). The predicted structure was validated by Ramachandran plot analysis in the Protein Structure Validation Suite (PSVS) (http://psvs-1_5-dev.nesg.org/). The position of two phosphate molecules analogous to Fru-2,6-P_2 in shrimp TIGAR was predicted by superimposition with the *D. rerio* 3D structure determined by X-ray diffraction (PDB: 3E9D, chain B) (2 Å)

[20]. The homology model was graphically analyzed and edited with PyMOL molecular graphics system (v. 1.8.2.0, Open-Source) (Schrödinger, LLC, New York, NY, USA).

2.5. Quantification of TIGAR mRNA relative expression by RT-qPCR

Total RNA was isolated from each tissue sample (~100 mg) from all the controls and treatments of the hypoxia experiment (see section 2.1.) with TRI Reagent (Sigma-Aldrich, St. Louis, MO, USA) according to manufacturer's protocol. The concentration and purity of RNA was evaluated by measuring the absorbance at 260 nm and the 260/280 ratio in a Nanodrop 2000c spectrophotometer (Thermo Scientific, Wilmington, DE, USA). The integrity of RNA was assessed by 1% agarose gel electrophoresis using Tris-acetate (TAE) buffer. Genomic DNA (gDNA) contamination was eliminated from total RNA with RNAse-free DNAse I (Roche, Mannheim, Germany) digestion. From each DNAse-treated RNA sample (0.5 µg), two cDNAs were synthesized in two separate reactions using the QuantiTect Reverse Transcription System (Quiagen, Valencia, CA, USA). Relative expression of TIGAR mRNA in cDNA samples was measured by quantitative PCR (qPCR). A TIGAR gene fragment (138 bp) was amplifyed using the specific primers TIGARFw1 and TIGARRv2 (Table S1). As reference to normalize TIGAR expression data, a fragment of the ribosomal protein L8 gene (166 bp) was amplified using the primers L8F2 and L8R2 (Table S1). The expression of L8 in the same white shrimp tissues during the same environmental conditions was validated as stable in a previous study [8]. The relative abundance of TIGAR mRNA in muscle, hepatopancreas and gills of shrimp under normal DO conditions were determined by qPCR in samples from normoxic control (24 h). As hepatopancreas is a main metabolic organ [24] and gills has many physiological functions [25], the effect of hypoxia on TIGAR expression was analyzed only in samples from these tissues. The expression of TIGAR and reference gene was analyzed in the two cDNA from each tissue sample in duplicated qPCR reactions (four technical replicates per shrimp). Each qPCR reaction (15 µL) included: 7.5 µL of 2x SyBr green qPCR Master Mix (Biotool, Houston, TX, USA), 1 µL of cDNA (corresponding to 25 ng of total RNA), and 0.5 µM of each TIGAR or L8 primer. A non-template control reaction was included in duplicate reactions per run to monitor reagent contamination. The reactions were performed in a CFX96 Touch Real-Time PCR Detection System (Bio-Rad, Hercules, CA, USA) under the following cycling conditions: 95 °C, 5 min (1 cycle); 95 °C, 30 s, 59.5 °C, 35 s, 72 °C, 55 s (40 cycles). The specificity of qPCR was evaluated by a melting curve analysis at the end of each run, in which the fluorescence was monitored from an interval from 65 to 95 °C with an increase of 0.3 °C each 5 s. The amplification efficiency for each qPCR product was estimated from a standard curve ($R^2 \geq 0.99$) obtained by plotting the quantification cycle (Cq) of serial dilutions of hepatopancreas cDNA (2.5×10^{1}–2.5×10^{-3} ng (derived from total RNA) for L8 or specific PCR product (5.0×10^{-3}-5.0×10^{-8} ng) for TIGAR. The standard curves were analyzed and graphically edited using CFX Manager 3.1 (Bio-Rad). The relative expression of each gene was calculated by the $2^{-\Delta Cq}$ method [26].

2.6. Statistics

Expression data was analyzed for normality and homoscedasticity by the Shapiro-Wilk and Levene's tests, respectively. As the data sets failed at least one test, non-parametric analyses were done. To assess statistical differences in mRNA abundance between tissues in normoxic conditions, Kruskal-Wallis test with Dunn's *post hoc* test was performed at a level of significance of $p \leq 0.05$. The same tests were done to stablish the effect of hypoxia on TIGAR expression in hepatopancreas and gills. Results were expressed as mean ± standard error of the mean (SEM). SigmaPlot 12 (Systat, San Jose, CA, USA) was used for statistical analyses and plots.

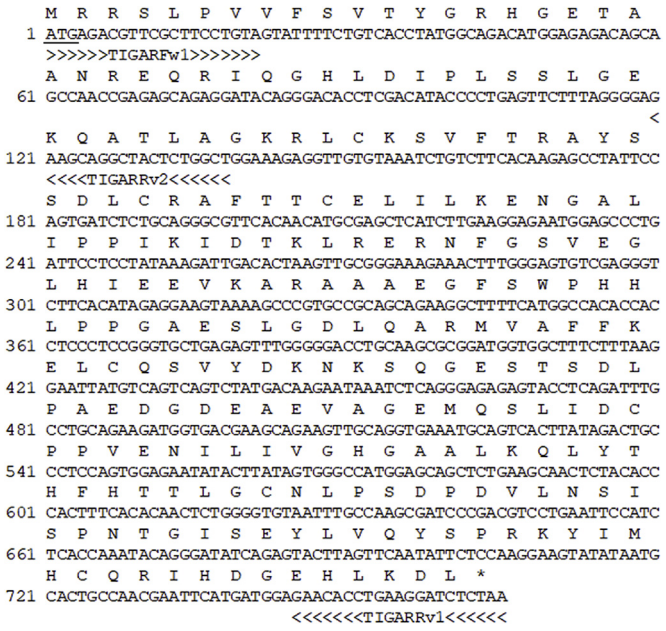

Fig. 1. Nucleotide and deduced amino acid sequence of *L. vannamei* TIGAR. The start codon is underlined and the stop codon is indicated by an asterisk. Position of forward and reverse specific primers used in this study are indicate as > and < .

3. Results and discussion

3.1. L. vannamei TIGAR cDNA

Using primers designed from a hepatopancreas TSA, we have cloned and sequenced a PCR product of 765 bp corresponding to the coding region of *L. vannamei* TIGAR cDNA (Fig. 1), which was submitted and annotated in the GenBank database (GenBank accession no. MK830070). The CDS starts with a methionine codon (ATG) and ends with an ochre stop codon (TAA). The sequence from this work has 99.74% identity to the sequence predicted from the TSA. The sequence obtained herein is also 99.06% identical to the CDS of a predicted TIGAR-like mRNA sequence (GenBank accession no. XM_027367713.1) from a recently annotated *L. vannamei* genome (GenBank Bioproject no. PRJNA508983). The TIGAR cDNA of *L. vannamei* encodes a protein of 254 amino acid residues with a theoretical MW of 28.1 kDa and pI of 6.0. Besides this white shrimp CDS, there are no other TIGAR-annotated and reported sequences from any penaeid shrimp or even decapod crustaceans in databases. Furthermore, as far we know, this is the first report documenting the presence of TIGAR homologs in invertebrate species.

3.2. Characterization of deduced shrimp TIGAR protein

The deduced amino acid sequence of *L. vannamei* TIGAR was compared with proteins from other animals by a multiple sequence alignment (Fig. 2). As expected, the shrimp protein shares the highest identities (Table 1) with other sequences from crustaceans like *A. vulgare* (49.2%) and the amphipod *H. gigas* (39.4%). In agreement, a phylogenetic analysis including proteins from diverse species (Fig. 3) clusters *L. vannamei* TIGAR with these two non-decapod species as indicated the high bootstrap value of the branch (99%). White shrimp TIGAR protein is also related to the homolog of water flea (59% of bootstrap value) as well as to the sequences of other non-crustacean arthropods like *Tetranychus urtica* and *Orchesella cincta* (58% of bootstrap value). As expected, vertebrate TIGAR sequences are clustered together with a high bootstrap value (99%). The vertebrate proteins are more related to those from mollusks such as *Mizuhopecten yessoensis* and

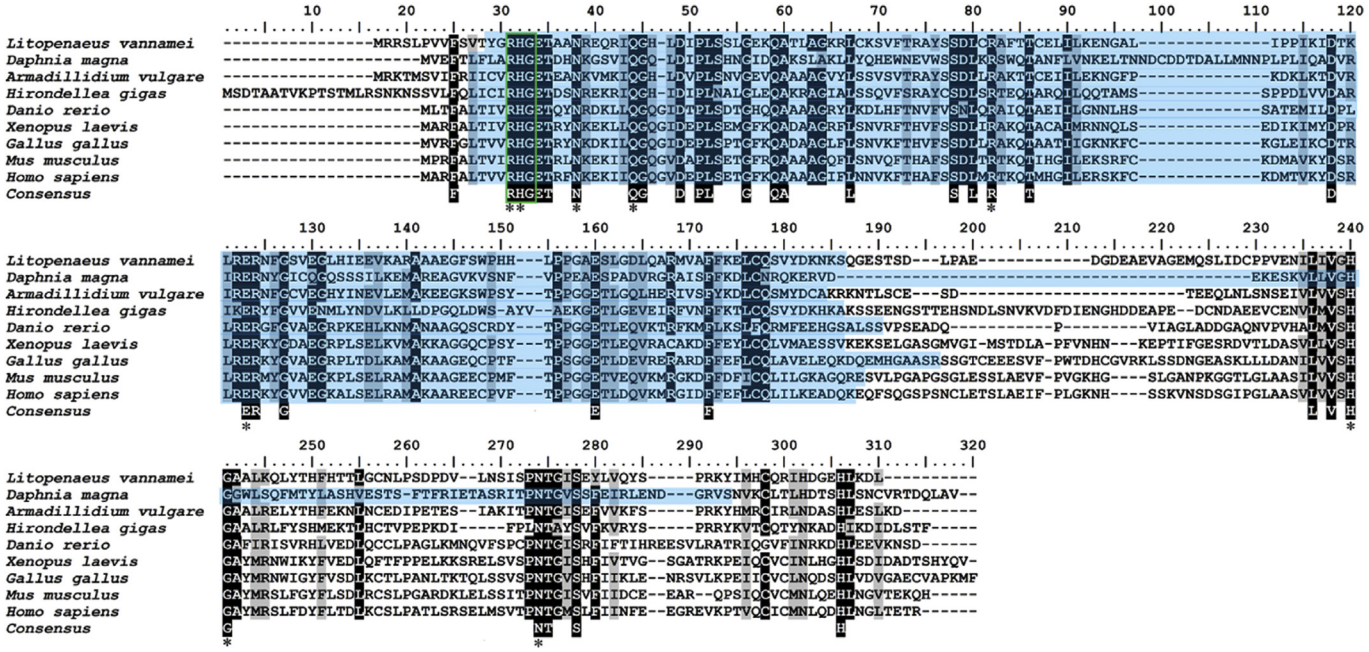

Fig. 2. Multiple sequence alignment of TIGAR proteins of different species. The histidine phosphatase superfamily (branch 1) domain is shaded in blue. The RHG motif is encased in green. Consensus, 100% sequence identity. The residues involved in Fru-2,6-P_2 binding in vertebrate TIGAR are indicated by an asterisk [21]. (For interpretation of the references to colour in this figure legend, the reader is referred to the Web version of this article.)

Crassostrea virginica (90% of bootstrap value) than to the sequences from arthropods.

Although the sequence identities are not so high (33.61%–35.34%, Table 1), TIGAR from *L. vannamei* presents the sequence features of vertebrate enzymes (Fig. 2). The histidine phosphatase (branch 1) superfamily domain (His_Phos_1) (Pfam: PF00300) containing the characteristic RHG motif [27] (R^{31}, H^{32}, G^{33}) was identified in all the sequences analyzed, including shrimp TIGAR (Fig. 2, Table 2). The predicted His_Phos_ 1 domain is 140 residues long in the white shrimp protein and has a similar length with the aligned proteins (140–154 residues), except for *D. magna* TIGAR that is longer (216 residues). The histidine phosphatase (branch 1) superfamily is a diverse group of enzymes that includes TIGAR and the bisphosphatase domain from the bifunctional PFK-2/FBPase-2, whose activity relies on the phosphorylation of a catalytic histidine residue in the RHG motif [27]. In addition, other residues involved in binding of substrates (for example, Fru-2,6-P_2) in vertebrate TIGAR (N^{38}, Q^{44}, R^{82}, E^{123}, H^{240}, G^{241}, N^{274}) [21] are identical in the *L. vannamei* protein (Fig. 2, Table 2).

The 3D structure of white shrimp TIGAR (Fig. 4) was predicted by homology modeling using the crystallographic structure of the *H. sapiens* enzyme as template, as it shares 35.15% sequence identity with a 88% of query coverage with the *L. vannamei* TIGAR. The root mean square deviation (RMSD) value obtained for the superimposed alpha carbon backbones of the model and template was 0.323 Å (< 1.5 Å), indicating that both structures are very similar [28]. The Ramachandran plot analysis revealed that only 0.9% of the residues in the shrimp model fell in disallowed regions, showing that the structure is stereochemically possible. In addition to human TIGAR, only the zebra fish structure has been experimentally determined [20], and it has 34.84% sequence identity with a 94% of query coverage to the *L. vannamei* TIGAR protein. The *D. rerio* crystallographic structure is also highly similar in folding to the *L. vannamei* homology model (RMSD = 0.639 Å) suggesting that the 3D structure is conserved between invertebrate and vertebrate TIGAR. As in *D. rerio* and *H. sapiens* structures, the two phosphate molecules analogous to substrate fit inside a cavity forming the active site (Fig. 4A) shaped by the catalytic important residues (Figs. 2 and 4B) [20,21].

The positions of alpha helices and beta-sheets predicted in the shrimp homology model (Fig. 5A) and human TIGAR (Fig. 5B) were compared to those reported in the zebra fish structure (Fig. 5C) [20]. Although the shared segments have slight variations in their length (≤4 residues) (Table 3), the number and distribution of helices and beta-sheets have some differences among the model and templates (Fig. 5, Table 3). For example, the α5 segment present in the vertebrate enzymes is absent in *L. vannamei* TIGAR. In contrast, the zebra fish crystallographic structure lacks the α8′ helix present in human TIGAR (eight residues long) and in the shrimp model (six residues long). Moreover, the predicted *L. vannamei* structure has a short C-terminal helix segment (α10, four residues long) present in *D. rerio* TIGAR (five residues long) but absent in the *H. sapiens* enzyme. Concerning to the

Table 1
Sequence identity (%) matrix of TIGAR proteins aligned using Clustal Omega.

	D. magna	*D. rerio*	*M. musculus*	*H. sapiens*	*X. laevis*	*G. gallus*	*H. gigas*	*L. vannamei*	*A. vulgare*
D. magna	100.00	28.51	32.44	32.74	32.61	35.65	29.28	32.88	33.94
D. rerio	28.51	100.00	41.90	40.00	47.06	43.53	31.43	33.61	35.71
M. musculus	32.44	41.90	100.00	72.76	50.37	55.02	28.19	34.98	39.83
H. sapiens	32.74	40.00	72.76	100.00	51.67	54.07	29.23	35.10	42.44
X. laevis	32.61	47.06	50.37	51.67	100.00	57.09	31.42	35.10	38.91
G. gallus	35.65	43.53	55.02	54.07	57.09	100.00	27.55	35.34	38.91
H. gigas	29.28	31.43	28.19	29.23	31.42	27.55	100.00	39.44	41.91
L. vannamei	32.88	33.61	34.98	35.10	35.10	35.34	39.44	100.00	49.17
A. vulgare	33.94	35.71	39.83	42.44	38.91	38.91	41.91	49.17	100.00

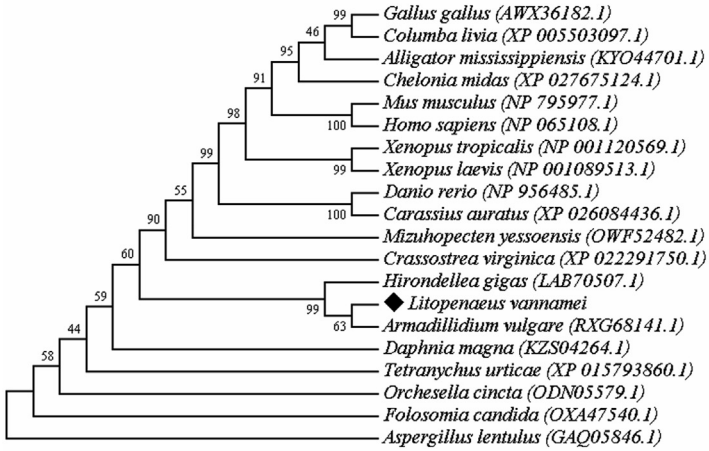

Fig. 3. Phylogenetic analysis of TIGAR amino acid sequences of various organisms. Twenty sequences were analyzed and 197 positions were considered in the final data set after the complete elimination of gaps. The tree was constructed by the ML method with the JTT matrix-based model. The numbers over each branch indicate the bootstrap value (%) estimated from 1000 replicates. The GenBank accession number of each sequence is in parenthesis.

beta-sheets, the *L. vannamei* model has less of these elements than the human and zebra fish TIGARs (eight and seven, respectively). The short β5 of zebra fish structure (three residues long) is absent in the shrimp and human proteins. In addition, the β1′ and β7' of *H. sapiens* TIGAR (both two residues long) are absent in the *L. vannamei* and *D. rerio* enzymes.

The structural similarity between vertebrate and shrimp TIGAR suggests that they may have similar enzyme activities in the cells. The ability of the zebra fish and human TIGAR to degrade Fru-2,6-P_2 has been demonstrated *in vitro* using recombinant proteins. TIGAR from those species may also use fructose-1,6-bisphosphate, the product of PFK-1 reaction. Degradation of any of these metabolites might reduce the glycolytic flux and increase the PPP rate [20]. It has been suggested that activation of PPP by TIGAR activity is reinforced by the stimulation of the gluconeogenic enzyme fructose 1,6-bisphosphatase (FBP), which is negatively regulated by Fru-2,6-P_2 levels [29]. On the other hand, TIGAR can use other substrates such as the glycolytic/gluconeogenic intermediates 2,3-bisphosphoglycerate, 2-phosphoglycerate and phosphoenolpyruvate with unknown metabolic consequences [30]. Therefore, it would be interesting to experimentally determine if the *L. vannamei* TIGAR presents such activities and their impact on carbohydrate flux through the central metabolic pathways in shrimp.

3.3. TIGAR expression during normoxia and hypoxia

The relative mRNA expression of *L. vannamei* TIGAR was analyzed by RT-qPCR. The amplification efficiencies of TIGAR and the reference gene L8 amplicons calculated from standard curves were 97% (Fig. S1). The abundance of TIGAR transcripts were statistically compared between hepatopancreas, gills and muscle in the normoxic control (24 h) (Fig. 6). The mRNA was significantly higher in gills than in hepatopancreas (by ~9-fold) ($p \leq 0.05$) and muscle (~5-fold) ($p \leq 0.05$). No significant differences were found between expression in hepatopancreas and muscle ($p \geq 0.05$). Although muscle and hepatopancreas are metabolically important organs and the main storage of carbohydrate, lipids and proteins in crustaceans [24], gills are crucial for physiological performance due to their vital roles in respiration,

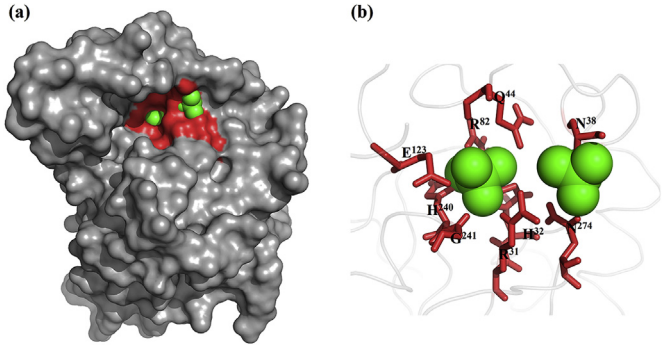

Fig. 4. *L. vannamei* TIGAR 3D structure. The shrimp structure was modeled from human TIGAR crystallographic structure (PDB: 3DCY, chain A). (a) Spatial distribution of active site (red) harboring two phosphate molecules (green) analogous to substrate in *L. vannamei* enzyme predicted from zebra fish crystallographic structure (PDB: 3E9D, chain B) [20]. (b) Residues (red) interacting with phosphate molecules (green) [21]. (For interpretation of the references to colour in this figure legend, the reader is referred to the Web version of this article.)

Table 2
Sequence features in the aligned proteins.

	Length of His_phos_1 domain[a] (residues)	RHG motif	Residues involved in Fru-2,6-P_2 binding[b]								
			R^{31}	H^{32}	N^{38}	Q^{44}	R^{82}	E^{123}	H^{240}	G^{241}	N^{274}
D. magna	216	+	+	+	+	+	+	+	+	+	+
D. rerio	148	+	+	+	+	+	+	+	+	+	+
M. musculus	146	+	+	+	+	+	+	+	+	+	+
H. sapiens	145	+	+	+	+	+	+	+	+	+	+
X. laevis	144	+	+	+	+	+	+	+	+	+	+
G. gallus	154	+	+	+	+	+	+	+	+	+	+
H. gigas	143	+	+	+	+	+	+	+	+	+	+
L. vannamei	140	+	+	+	+	+	+	+	+	+	+
A. vulgare	140	+	+	+	+	+	+	+	+	+	+

+, present.
[a], Pfam: PF00300.
[b], according to reports in vertebrates.

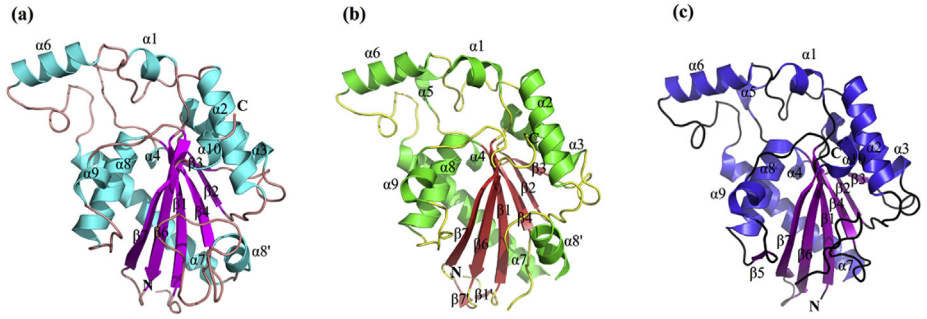

Fig. 5. Comparative ribbon diagrams for secondary structures of white shrimp and vertebrate TIGAR. (a) *L. vannamei* (homology model), (b) *H. sapiens* (template structure, PDB: 3DCY, chain A) and (c) *D. rerio* (PDB: 3E9D, chain B). In all: N, N-terminus; C, C-terminus. Position alpha helices (α) and beta-sheets (β) are indicated relative to *D. rerio* structure [20].

Table 3
Length (residues) and total number of alpha helices (α) and beta-sheets (β) in *L. vannamei*, *H. sapiens* and *D. rerio* TIGAR structures.

Secondary structure	*L. vannamei*	*H. sapiens*	*D. rerio*
α1	5	7	6
α2	15	15	15
α3	13	13	14
α4	3	4	4
α5	–	5	5
α6	11	12	12
α7	24	26	25
α8′	6	8	–
α8	15	15	14
α9	5	7	6
α10	4	–	5
Total α	10	10	10
β1′	–	2	–
β1	9	9	9
β2	4	4	4
β3	3	3	3
β4	7	6	6
β5	–	–	3
β6	10	8	10
β7′	–	2	–
β7	10	9	13
Total β	6	8	7

-, absent.

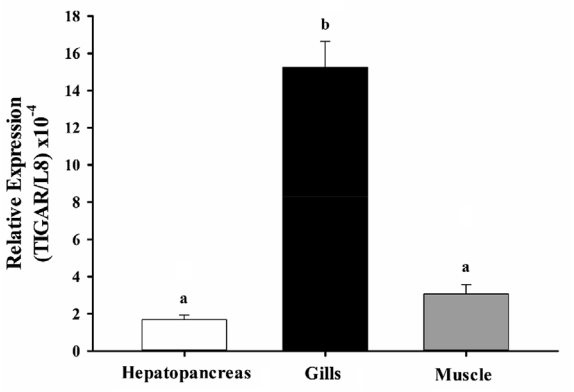

Fig. 6. Expression of white shrimp TIGAR in different tissues under normoxia. Data are expressed as mean ± SEM ($n = 4$). Significant differences ($p \leq 0.05$) between tissues are indicated by letters.

detoxification, excretion and osmoregulation [25]. In addition, gills are physically in contact with the aquatic medium, thus their cells are constantly exposed to environmental changes [31]. Therefore, the maintenance of relatively high levels of proteins involved in stress tolerance like TIGAR, even under optimal environmental conditions, must be critical for shrimp upon the encounter of stressful situations.

Because hypoxia is a common stressor affecting shrimp culture [3], we examined the effect of reduced oxygen concentration (~1.5 mg L^{-1}) on TIGAR expression. According to our results, TIGAR expression responds to hypoxic stress in hepatopancreas (Fig. 7a) and gills (Fig. 7b). TIGAR mRNA was significantly up-regulated by ~10-fold in hepatopancreas after 24–48 h of exposure compared to the normoxic control. In gills, TIGAR expression significantly increased by ~3-fold in response to 24 h of hypoxia. However, after 48 h transcripts abundance in hypoxic shrimp was significantly lower than in animals under normoxia by ~3-fold. These results showed that TIGAR is regulated by hypoxia in *L. vannamei* with a tissue-specific pattern of response.

As FBPase-2, TIGAR downregulates glycolysis [19], which in a strict sense, is disadvantageous for hypoxic cells that heavily rely on this pathway for ATP production. However, up-regulation of TIGAR has been demonstrated in mammalian cells exposed to hypoxia or ischemia-reperfusion injury [32–34]. In some cell lines, a fraction of the TIGAR protein is translocated to the mitochondria and there associates with the enzyme HK-2, resulting in the enhancement of HK-2 activity, and the lowering of mitochondrial ROS, in an independent way to its bisphosphatase activity, which also contributes to decrease ROS in cells through the stimulation of PPP [23]. Furthermore, activation of PPP is considered the fastest way to optimize the cellular redox state and survive oxidative stress [35]. Overexpression of TIGAR in ischemic mice tissues boosts glucose-6-phosphate dehydrogenase expression, the rate limiting step of PPP [34]. Increase in PPP leads to rises in NADPH and GSH, hence reducing ROS-induced apoptosis, suggesting that TIGAR is involved in the tolerance to ischemic injury [36]. Similarly, TIGAR up-regulation could contribute to the survival of shrimp cells during hypoxic episodes by some or all of these mechanisms.

In *L. vannamei*, HIF-1 dependent induction of glycolytic enzymes occurs in the first stages of the exposure to moderate hypoxia [6,7,10,11]. Interestingly, in hepatopancreas, acceleration of glycolysis under hypoxia, evidenced by increases in PFK expression and activity but also by tissue lactate accumulation, takes place with a nearly concomitant up-regulation of the gluconeogenic enzyme FBP *via* HIF-1 [8,10]. Against the economy of cells during hypo-metabolism, activation of gluconeogenesis as an energy-consuming process could be beneficial as a way to shunt glycolytic intermediaries towards PPP to replenish cells NADPH and nucleotide precursors [8]. This would help to counteract the oxidative damage in biomolecules like DNA and lipids that has been shown to affect shrimp tissues during hypoxic and post-hypoxic stress [37]. Thus, TIGAR could be an important dual control point of glycolytic/gluconeogenic rates by modulating PFK/FBP activity to avoid oxidative damage and cell death in shrimp during episodic hypoxia, but also may play a role in the preparation of antioxidant defenses to reduce oxidative damage when reoxygenation happens, as has been previously theorized to occur in shrimp and other benthic animals [38]. Therefore, HIF-1 could be involved in mechanisms regulating TIGAR functions, since the abundance of the oxygen-regulated HIF-1α subunit transcript is induced in gills [11] and hepatopancreas [10] during 24–48 h of hypoxia (~1.5 mg L^{-1}). In addition to two p53 response elements, the human TIGAR gene promoter presents six putative hypoxia response elements for HIF-1 binding and at least one of

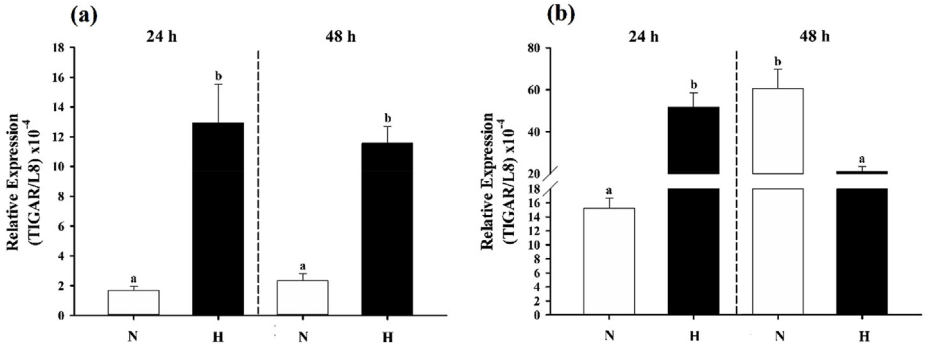

Fig. 7. Effect of hypoxia on TIGAR expression. (a) Hepatopancreas and (b) Gills. In both: normoxia (N); hypoxia (H). Data are expressed as mean ± SEM ($n = 4$). Significant differences ($p \leq 0.05$) in each tissue are indicated by letters.

them has been shown to be functional [39], thus suggesting that the shrimp TIGAR gene could be directly regulated by p53 and HIF-1. This could be addressed by the sequencing of the TIGAR gene promoter and the search of functional HIF-1 and p53 binding sites by promoter activity assays, in combination with the analysis of TIGAR expression when these transcription factors are silenced by RNA interference or site-directed mutagenesis.

In contrast, p53-dependent induction of TIGAR can act as a pro-apoptotic stimulus as has been demonstrated in mammalian cardiomyocytes under hypoxia [33]. When cellular damage caused by ROS is irreparable, programmed cell death is activated [40]. In white shrimp, long-term exposure to hypoxia (days) increases apoptosis in hemocytes and hepatopancreas [16,17]. In this tissues, the expression or activity of the effector Caspase-3 increases in response to hypoxia and those changes do not occur when p53 expression is silenced [16,17]. This suggest that in a similar way to mammalian cells, p53 is important to decide cell fate during hypoxic stress in shrimp. As we detected TIGAR induction in gills after 48 h of exposure to low DO, it is possible that it is involved in the apoptotic response in shrimp cells under long-term hypoxia. However, the effects of p53 and TIGAR on cell fate in vertebrates are complex and depend on factors like cell-type, nutrition and redox state [39]. In addition, we detected the up-regulation of TIGAR expression in gills after 48 h of normoxia, indicated that it may be regulated in shrimp by other stimuli under normal oxygen conditions. Therefore, the potential roles of TIGAR in *L. vannamei* must be explored in defined contexts for tissue-type, stressor, duration and intensity of insults.

4. Conclusions

In conclusion, we obtained a nucleotide sequence encoding *L. vannamei* TIGAR and the deduced protein was characterized using bioinformatics tools. Shrimp TIGAR conserves the amino acid residues determinant for bisphosphatase activity found in the enzymes from vertebrates, suggesting that it may have similar functions. Those findings were supported by the high structural similarity of shrimp TIGAR and the proteins from human and zebra fish predicted by homology modeling. Gene expression analysis showed that *L. vannamei* TIGAR under normal DO conditions is mainly expressed in gills, and is regulated by hypoxia in hepatopancreas and gills, suggesting its involvement in the cellular response to stress caused by environmental oxygen fluctuations. Further experiments are necessary to determine TIGAR enzymatic activities, physiological effects and the molecular mechanisms controlling its expression in white shrimp cells under hypoxia.

Author contributions

LCJ and GYP conceived and designed experiments. LCJ, MFP and DMNH performed experiments. LCJ analyzed the data and drafted the manuscript. All the authors critically revised and approved the final version of the manuscript.

Conflicts of interest

The authors declare no competing or financial interests.

Acknowledgments

This research was funded by CONACyT grants PN 2017/4869 and A1-S-24557 to GYP. LCJ has a CONACyT postdoctoral fellowship. We specially thank Dr. Silvia Gomez-Jimenez and the personnel from the Laboratory of Marine Invertebrates Physiology of CIAD for their technical assistance during the biological assays.

Appendix A. Supplementary data

Supplementary data to this article can be found online at https://doi.org/10.1016/j.fsi.2019.08.003.

References

[1] R.J. Diaz, Overview of hypoxia around the world, J. Environ. Qual. 30 (2001) 275, https://doi.org/10.2134/jeq2001.302275x.
[2] W.Y.B. Chang, H.A.I. Ouyang, Dynamics of dissolved oxygen and vertical circulation in fish ponds, Aquaculture 74 (1988) 263–276, https://doi.org/10.1016/0044-8486(88)90370-5.
[3] C.I. Pérez-Rostro, I.S. Racotta, A.M. Ibarra, Decreased genetic variation in metabolic variables of *Litopenaeus vannamei* shrimp after exposure to acute hypoxia, J. Exp. Mar. Biol. Ecol. 302 (2004) 189–200, https://doi.org/10.1016/j.jembe.2003.10.010.
[4] S. Han, B. Wang, M. Liu, M. Wang, K. Jiang, C. Qi, L. Wang, Effect of cyclic serious/medium hypoxia stress on the survival, growth performance and resistance against *Vibrio parahemolyticus* of white shrimp *Litopenaeus vannamei*, Invertebr. Surviv. J. 14 (2017) 259–270.
[5] D. Hoogewijs, N.B. Terwilliger, K.A. Webster, J.A. Powell-Coffman, S. Tokishita, H. Yamagata, T. Hankeln, T. Burmester, K.T. Rytknen, M. Nikinmaa, D. Abele, K. Heise, M. Lucassen, J. Fandrey, P.H. Maxwell, S. Phlman, T.A. Gorr, From critters to cancers: bridging comparative and clinical research on oxygen sensing, HIF signaling, and adaptations towards hypoxia, Integr. Comp. Biol. 47 (2007) 552–577, https://doi.org/10.1093/icb/icm072.
[6] J.G. Soñanez-Organis, A.B. Peregrino-Uriarte, R.R. Sotelo-Mundo, H.J. Forman, G. Yepiz-Plascencia, Hexokinase from the white shrimp *Litopenaeus vannamei*: cDNA sequence, structural protein model and regulation via HIF-1 in response to hypoxia, Comp. Biochem. Physiol. B Biochem. Mol. Biol. 158 (2011) 242–249, https://doi.org/10.1016/j.cbpb.2010.12.006.
[7] J.G. Soñanez-Organis, M. Rodriguez-Armenta, B. Leal-Rubio, A.B. Peregrino-Uriarte, S. Gómez-Jiménez, G. Yepiz-Plascencia, Alternative splicing generates two lactate dehydrogenase subunits differentially expressed during hypoxia via HIF-1 in the shrimp *Litopenaeus vannamei*, Biochimie 94 (2012) 1250–1260, https://doi.org/10.1016/j.biochi.2012.02.015.
[8] K. Cota-Ruiz, A.B. Peregrino-Uriarte, M. Felix-Portillo, J.A. Martínez-Quintana, G. Yepiz-Plascencia, Expression of fructose 1,6-bisphosphatase and phospho-fructokinase is induced in hepatopancreas of the white shrimp *Litopenaeus vannamei* by hypoxia, Mar. Environ. Res. 106 (2015) 1–9, https://doi.org/10.1016/j.marenvres.2015.02.003.
[9] L. Camacho-Jiménez, A.B.A.B. Peregrino-Uriarte, J.A.J.A. Martínez-Quintana, G. Yepiz-Plascencia, The glyceraldehyde-3-phosphate dehydrogenase of the shrimp *Litopenaeus vannamei*: molecular cloning, characterization and expression during

hypoxia, Mar. Environ. Res. 138 (2018) 65–75, https://doi.org/10.1016/j.marenvres.2018.04.003.
[10] K. Cota-Ruiz, L. Leyva-carrillo, A.B. Peregrino-uriarte, E.M. Valenzuela-Soto, T. Gollas-Galván, S. Gómez-Jiménez, J. Hernández, G. Yepiz-Plascencia, Role of HIF-1 on phosphofructokinase and fructose 1,6-bisphosphatase expression during hypoxia in the white shrimp *Litopenaeus vannamei*, Comp. Biochem. Physiol., A 198 (2016) 1–7, https://doi.org/10.1016/j.cbpa.2016.03.015.
[11] L. Camacho-Jiménez, L. Leyva-Carrillo, A.B. Peregrino-Uriarte, J.L. Duarte-Gutiérrez, M. Tresguerres, G. Yepiz-plascencia, Regulation of glyceraldehyde-3-phosphate dehydrogenase by hypoxia inducible factor 1 in the white shrimp *Litopenaeus vannamei* during hypoxia and reoxygenation, Comp. Biochem. Physiol., A (2019), https://doi.org/10.1016/j.cbpa.2019.05.006.
[12] T.A. Gorr, M. Gassmann, P. Wappner, Sensing and responding to hypoxia via HIF in model invertebrates, J. Insect Physiol. 52 (2006) 349–364, https://doi.org/10.1016/j.jinsphys.2006.01.002.
[13] A. Sermeus, C. Michiels, Reciprocal influence of the p53 and the hypoxic pathways, Cell Death Dis. 2 (2011) e164, https://doi.org/10.1038/cddis.2011.48.
[14] O.D.K. Maddocks, K.H. Vousden, Metabolic regulation by p53, J. Mol. Med. 89 (2011) 237–245, https://doi.org/10.1007/s00109-011-0735-5.
[15] S. Sun, Z. Gu, H. Fu, J. Zhu, X. Ge, F. Xuan, Molecular cloning, characterization, and expression analysis of p53 from the oriental river prawn, *Macrobrachium nipponense*, in response to hypoxia, Fish Shellfish Immunol. 54 (2016) 68–76, https://doi.org/10.1016/j.fsi.2016.03.167.
[16] M. Felix-Portillo, J.A. Martínez-Quintana, M. Arenas-Padilla, V. Mata-Haro, S. Gómez-Jiménez, G. Yepiz-Plascencia, Hypoxia drives apoptosis independently of p53 and metallothionein transcript levels in hemocytes of the whiteleg shrimp *Litopenaeus vannamei*, Chemosphere 161 (2016) 454–462, https://doi.org/10.1016/j.chemosphere.2016.07.041.
[17] D.M. Nuñez-Hernandez, M. Felix-Portillo, A.B. Peregrino-Uriarte, G. Yepiz-Plascencia, Cell cycle regulation and apoptosis mediated by p53 in response to hypoxia in hepatopancreas of the white shrimp *Litopenaeus vannamei*, Chemosphere 190 (2018) 253–259, https://doi.org/10.1016/j.chemosphere.2017.09.131.
[18] Y. Itahana, K. Itahana, Emerging roles of p53 family members in glucose metabolism, Int. J. Mol. Sci. 19 (2018), https://doi.org/10.3390/ijms19030776.
[19] K. Bensaad, A. Tsuruta, M.A. Selak, M.N.C. Vidal, K. Nakano, R. Bartrons, E. Gottlieb, K.H. Vousden, TIGAR, a p53-inducible regulator of glycolysis and apoptosis, Cell 53 (2006) 107–120, https://doi.org/10.1016/j.cell.2006.05.036.
[20] H. Li, G. Jogl, Structural and biochemical studies of TIGAR (TP53-induced glycolysis and apoptosis regulator), J. Biol. Chem. 284 (2009) 1748–1754, https://doi.org/10.1074/jbc.M807821200.
[21] J. Geng, X. Yuan, M. Wei, J. Wu, Z. Qin, The diverse role of TIGAR in cellular homeostasis and cancer, Free Radic. Res. 52 (2018) 1240–1249, https://doi.org/10.1080/10715762.2018.1489133.
[22] P. Lee, K.H. Vousden, E.C. Cheung, T.I.G.A.R. TIGAR, Burning bright, Cancer Metabol. 2 (2014), https://doi.org/10.1186/2049-3002-2-1.
[23] E.C. Cheung, R.L. Ludwig, K.H. Vousden, Mitochondrial localization of TIGAR under hypoxia stimulates HK2 and lowers ROS and cell death, Proc. Natl. Acad. Sci. U.S.A. 109 (2012), https://doi.org/10.1073/pnas.1206530109.
[24] A.G. Jimenez, S.T. Kinsey, Energetics and metabolic regulation, first ed., in: E.S. Chang, M. Thiel (Eds.), Nat. Hist. Crustac. vol. 4, Oxford University Press, New York, 2015, pp. 391–419 Physiol.
[25] R.P. Henry, C. Lucu, H. Onken, D. Weihrauch, Multiple functions of the crustacean gill: osmotic/ionic regulation, acid-base balance, ammonia excretion, and bioaccumulation of toxic metals, Front. Physiol. 3 (2012), https://doi.org/10.3389/fphys.2012.00431.
[26] T.D. Schmittgen, K.J. Livak, Analyzing real-time PCR data by the comparative CT method, Nat. Protoc. 3 (2008) 1101–1108.
[27] D.J. Rigden, The histidine phosphatase superfamily : structure and function, Biochem. J. 348 (2008) 333–348, https://doi.org/10.1042/BJ20071097.
[28] D. Sheehan, S. O'Sullivan, Online homology modelling as a means of bridging the sequence-structure gap, Bioengineered Bugs 2 (2011) 299–305, https://doi.org/10.4161/bbug.2.6.16116.
[29] S. Ros, A. Schulze, Balancing glycolytic flux: the role of 6-phosphofructo-2-kinase/fructose 2,6-bisphosphatases in cancer metabolism, Cancer Metabol. 1 (2013) 8, https://doi.org/10.1186/2049-3002-1-8.
[30] I. Gerin, G. Noël, J. Bolsée, O. Haumont, E. Van Schaftingen, G.T. Bommer, Identification of TP53-induced glycolysis and apoptosis regulator (TIGAR) as the phosphoglycolate-independent 2,3-bisphosphoglycerate phosphatase, Biochem. J. 448 (2014) 439–448, https://doi.org/10.1042/BJ20130841.
[31] A. Clavero-Salas, R.R. Sotelo-Mundo, T. Gollas-Galván, J. Hernández-López, A.B. Peregrino-Uriarte, A. Muhlia-Almazán, G. Yepiz-Plascencia, Transcriptome analysis of gills from the white shrimp *Litopenaeus vannamei* infected with White Spot Syndrome Virus, Fish Shellfish Immunol. 23 (2007) 459–472, https://doi.org/10.1016/j.fsi.2007.01.010.
[32] J. Kim, K. Devalaraja-narashimha, B.J. Padanilam, TIGAR regulates glycolysis in ischemic kidney proximal tubules, Am. J. Ren. Physiol. 308 (2015) F298–F308, https://doi.org/10.1152/ajprenal.00459.2014.
[33] M. Kimata, S. Matoba, E. Iwai-kanai, H. Nakamura, A. Hoshino, M. Nakaoka, p53 and TIGAR regulate cardiac myocyte energy homeostasis under hypoxic stress, Am. J. Physiol. Heart Circ. Physiol. 299 (2010) H1908–H1916, https://doi.org/10.1152/ajpheart.00250.2010.
[34] M. Li, M. Sun, L. Cao, J. Gu, J. Ge, J. Chen, R. Han, Y. Qin, Z. Zhou, Y. Ding, Z. Qin, TIGAR-regulated metabolic pathway is critical for protection of brain schemia, J. Neurosci. 34 (2014) 7458–7471, https://doi.org/10.1523/JNEUROSCI.4655-13.2014.
[35] T.P. Dick, M. Ralser, Metabolic remodeling in times of stress: who shoots faster than His shadow? Mol. Cell 59 (2015) 519–521, https://doi.org/10.1016/j.molcel.2015.08.002.
[36] J. Zhou, T. Zhang, D. Song, Y. Xia, Z. Qin, R. Sheng, TIGAR contributes to ischemic tolerance induced by cerebral preconditioning through scavenging of reactive oxygen species and inhibition of apoptosis, Sci. Rep. 3 (2016) 1–11, https://doi.org/10.1038/srep27096.
[37] Y. Li, L. Wei, J. Cao, L. Qiu, X. Jiang, P. Li, Q. Song, H. Zhou, Q. Han, X. Diao, Oxidative stress, DNA damage and antioxidant enzyme activities in the pacific white shrimp (*Litopenaeus vannamei*) when exposed to hypoxia and reoxygenation, Chemosphere 144 (2016) 234–240, https://doi.org/10.1016/j.chemosphere.2015.08.051.
[38] M. Giraud-billoud, G.A. Rivera-ingraham, D.C. Moreira, T. Burmester, A. Castro-vazquez, J.M. Carvajalino-fernández, A. Dafre, C. Niu, B. Paital, R. Rosa, J.M. Storey, A. Vega, W. Zhang, G. Yepiz-plascencia, T. Zenteno, K.B. Storey, M. Hermes-lima, Twenty years of the 'Preparation for Oxidative Stress' (POS) theory: ecophysiological advantages and molecular strategies, Comp. Biochem. Physiol., A (2019), https://doi.org/10.1016/j.cbpa.2019.04.004.
[39] R. Rajendran, R. Garva, H. Ashour, T. Leung, I.A.N. Stratford, M. Krstic-demonacos, C. Demonacos, Acetylation mediated by the p300/CBP-associated factor determines cellular energy metabolic pathways in cancer, Int. J. Oncol. 42 (2013) 1961–1972, https://doi.org/10.3892/ijo.2013.1907.
[40] M. Ott, V. Gogvadze, S. Orrenius, B. Zhivotovsky, Mitochondria, oxidative stress and cell death, Apoptosis 12 (2007) 913–922, https://doi.org/10.1007/s10495-007-0756-2.